

## Raman scattering observations and *ab initio* models of dicarbon complexes in AlAs

B. R. Davidson\* and R. C. Newman

*Interdisciplinary Research Centre for Semiconductor Materials, The Blackett Laboratory, Imperial College of Science, Technology and Medicine, London SW7 2BZ, United Kingdom*

C. D. Latham and R. Jones

*Department of Physics, University of Exeter, Exeter EX4 4QL, United Kingdom*

J. Wagner

*Fraunhofer-Institut für Angewandte Festkörperphysik, Tullastrasse 72, D-71908 Freiburg, Federal Republic of Germany*

C. C. Button

*Department of Electronic and Electrical Engineering, University of Sheffield, Mappin Street, Sheffield S1 3JD, United Kingdom*

P. R. Briddon

*Department of Physics, The University of Newcastle upon Tyne, Newcastle upon Tyne NE1 7RU, United Kingdom*  
(Received 22 April 1999)

Raman scattering from an as-grown or annealed AlAs carbon  $\delta$ -doping superlattice reveals lines at 1752 and 1856  $\text{cm}^{-1}$ : the latter line shows the weaker intensity but has a resonant enhancement for incident light with an energy of 3 eV. These lines are comparable with those assigned to vibrational modes of two directly bonded dicarbon centers in GaAs [J. Wagner *et al.*, Phys. Rev. Lett. **78**, 74 (1997)]. First principles calculations are carried out to determine the structure and vibrational modes of dicarbon C-C defects located at various substitutional and interstitial sites in both AlAs and GaAs. The frequency of the C-C stretch mode is sensitive to the charge state and orientation and errors are not expected to exceed 10%. The dicarbon complex centered at an arsenic site is a deep donor and in its positively charged state is found to have axes aligned close to either  $\langle 110 \rangle$  or  $\langle 111 \rangle$  directions. The calculated frequencies and energies for the two orientations are essentially the same, so that these two structures offer an explanation for the observation of the two dicarbon Raman modes. An alternative assignment of one of the two observed modes to a different defect, such as an interstitial complex or neutral substitutional dimers, are considered but are ruled out as being incompatible with the experimental observations. [S0163-1829(99)04232-0]

### I. INTRODUCTION

There has been considerable interest in the use of carbon as a *p*-type dopant in epitaxial GaAs and related compounds.<sup>1</sup> However, the reduction in the hole concentration, *p*, in the binary III-V compound GaAs that is heavily doped with carbon ( $[\text{C}] > 10^{20} \text{ cm}^{-3}$ ) after it has been annealed at a high temperature, typically close to 850 °C, is now well established. This reduction is initially accompanied by a drop in carrier mobility but after prolonged anneals the mobility has been observed to increase again. This behavior indicates that the first step is the formation of compensating defects (donors or hole traps) (Ref. 2) but electrically inactive defects, such as clusters, form if the heat treatment is extended.<sup>3</sup> The existence of C-C pairs in annealed epilayers was later demonstrated by Raman scattering measurements made on GaAs samples that contained both <sup>12</sup>C and <sup>13</sup>C isotopes: two triplet structures (*T1* and *T2*) were observed, which were attributed to different C-C complexes.<sup>4</sup> Consistent with these observations, this study also revealed a loss of substitutional carbon. It is implied that carbon atoms are displaced into interstitial sites, possibly by the capture of mobile arsenic interstitials or alternatively with the formation of arsenic vacancies. The latter centers are known to act as hole

traps but we are unaware of a spectroscopic method of detecting these vacancies. There could, therefore, be formation of C-C complexes with an adjacent arsenic vacancy.

Prior to these Raman studies, *ab initio* calculations<sup>5,6</sup> of a directly bonded dicarbon split interstitial located at an As lattice site predicted that this complex is a deep donor and would be in the positive charge state in *p*-type GaAs and AlAs; thus formation of these C-C pairs during annealing would contribute to the reduction in electrical activity. Subsequent calculations for C-C pairs in GaAs allowed comparisons to be made with the measured stretch frequencies of the *T1* and *T2* centers.<sup>4</sup> Preliminary calculations carried out for neutral dimers located in an interstitial cage comprising four As atoms yielded local vibrational mode (LVM) frequencies close to those of the *T2* center.

We note that although the Raman results for the mixed isotope GaAs sample showed two triplets, it is not essential that the two carbon atoms comprising the dimers that give rise to these modes should be equivalent if the splitting between the frequencies of the modes for the two configurations of <sup>12</sup>C-<sup>13</sup>C is too small to be resolved experimentally. However, the linewidths of the mixed isotope modes might be expected to be measurably broader than the pure <sup>12</sup>C and <sup>13</sup>C lines. This possibility was investigated by comparing the

measured spectra with simulations using Lorentzian line shapes. It was found that for the slightly sharper  $T1$  line, the splitting would need to be at least  $5\text{ cm}^{-1}$  for broadening to be observed, and  $\geq 10\text{ cm}^{-1}$  for the  $T2$  line.

Heavy doping of GaAs with carbon has been studied because of its use in heterojunction bipolar transistors (HBTs), since high doping levels are required to obtain a low series resistance of the base region. A second requirement for high  $p$ -type doping is in AlAs, rather than GaAs, for application in vertical-cavity surface-emitting lasers (VCSELs) that use AlAs/GaAs distributed Bragg reflectors (DBRs): again there is a requirement to minimize the electrical resistance associated with the multiple heterojunctions in the  $p$ -type DBR.<sup>7</sup> If carbon doping is used there is a question of whether or not all the carbon is electrically active since dicarbon complexes may form, similar to those found in annealed GaAs. First, we briefly review the available literature relating to heavy carbon doping in  $\text{Al}_x\text{Ga}_{1-x}\text{As}$  and AlAs.

The reported behavior of heavily carbon-doped  $\text{Al}_x\text{Ga}_{1-x}\text{As}$  for values of  $x$  less than 0.22 is similar to that observed for GaAs:C. Annealing at temperatures above  $600\text{ }^\circ\text{C}$  leads to decreases in  $p$  due to the formation of compensating centers, which also leads to decreases in the strain.<sup>8–11</sup> However, a 5 min anneal at  $950\text{ }^\circ\text{C}$  in a He ambient of an AlAs layer with  $p \sim 10^{20}\text{ cm}^{-3}$  produced a smaller decrease in  $p$  than that of a corresponding anneal of similarly doped GaAs:C. Attempts to obtain  $[\text{C}] > 1 \times 10^{20}\text{ cm}^{-3}$  by using  $\text{CCl}_4$  or  $\text{CBr}_4$  to dope AlAs during growth by metal-organic molecular beam epitaxy (MOMBE) led to highly compensated material. This was not due exclusively to the incorporation of  $\text{H-C}_{\text{As}}$  pairs and it was suggested, but without direct evidence, that C-C pairs had been formed.<sup>11</sup> No evidence of relaxation or the presence of precipitates was obtained by transmission electron microscopy (TEM) nor were interstitials detected by Rutherford backscattering or LVM spectroscopy. Carbon doping of AlAs by solid source molecular beam epitaxy (SSMBE) leads to the incorporation of C in forms other than electrically active acceptors so that  $p$  is less than the carbon concentration  $[\text{C}]$ .<sup>12</sup> This probably results from the incorporation of carbon as dimers and larger clusters, as also inferred for SSMBE of GaAs and  $\text{Al}_x\text{Ga}_{1-x}\text{As}$ , as it is known that these species evaporate from the incandescent graphite filament as well as individual C atoms.<sup>13</sup> There is, however, no spectroscopic or microscopic evidence to our knowledge that shows how these clusters are incorporated into the lattice. Nevertheless, low-resistance  $p$ -type DBRs have been grown by SSMBE, by combining C-doped AlAs with Be-doped GaAs.<sup>14</sup>

In summary, for AlAs doped with  $[\text{C}] > 10^{20}\text{ cm}^{-3}$  it is evident that not all the C is necessarily incorporated as shallow acceptors and compensating carbon complexes can form either during growth or annealing. In Sec. II, we report new Raman scattering and infrared measurements on as-grown and annealed AlAs containing carbon acceptors grown by metal-organic vapor phase epitaxy (MOVPE) using  $\text{CCl}_4$  as a carbon source and demonstrate that dicarbon complexes are formed corresponding to those detected previously in GaAs. In Sec. III, the details and results of first principles calculations relating to the structure and the LVMs of dicarbon complexes are presented. It is found that the orientation of a carbon dimer occupying an As site in either GaAs or AlAs is

dependent on its charge state. The axis of the positively charged defect is oriented along a  $\langle 110 \rangle$  or a  $\langle 111 \rangle$  direction, whereas the neutral defect has the lowest energy when its axis is close to a  $\langle 100 \rangle$  direction but a Jahn-Teller distortion lowers the  $D_{2d}$  symmetry. Defects in both charge states give rise to high-frequency LVMs. Other configurations, including the interstitial caged dimer, have also been investigated. We compare and discuss the experimental and theoretical results in Sec. IV and our conclusions are given in Sec. V.

## II. EXPERIMENTAL INVESTIGATION

### A. Sample preparation

Previous Raman measurements of GaAs:C have shown that grown-in carbon concentrations greater than  $10^{20}\text{ cm}^{-3}$  are required in order for detectable concentrations of dicarbon complexes to form during annealing. To avoid having GaAs in direct contact with highly doped AlAs, which might lead to a similar high doping level in the GaAs close to the interface, we examined an AlAs carbon  $\delta$ -doping superlattice structure (labeled MR685). This was grown by MOVPE using trimethylgallium, trimethylaluminum (TMAl), and arsine precursors, together with carbon tetrachloride for intentional carbon doping.

In more detail, a nominally undoped GaAs buffer layer of thickness 300 nm was deposited onto the undoped semi-insulating GaAs substrate misoriented  $4^\circ$  off (100) towards (110), followed by a 50 nm thick AlAs layer that was uniformly doped to a concentration of  $[\text{C}_{\text{As}}] \sim 10^{19}\text{ cm}^{-3}$ , with the carbon derived from the TMAl. A heavily carbon-doped thin layer ( $\delta$  doped) was then obtained by introducing  $\text{CCl}_4$  into the reactor for a period of 2 s without interrupting the growth. This was followed by the growth of a spacer layer of 50 nm of intrinsically doped AlAs. This sequence was repeated 50 times to generate the  $\delta$ -doping superlattice. The growth rate was  $0.6\text{ nm s}^{-1}$ , which implies an intended minimum thickness of the  $\delta$ -doping layers of 1.2 nm. Finally, a nominally undoped GaAs capping layer was grown with a thickness of 20 nm. The growth temperature was  $620\text{ }^\circ\text{C}$  and a low arsine flow was used to enhance carbon incorporation. After growth, parts of the wafer were annealed in a nitrogen atmosphere at  $600\text{ }^\circ\text{C}$  for 15 min to remove grown-in hydrogen. Some of this material was subsequently annealed at  $850\text{ }^\circ\text{C}$  for 30 min in an argon atmosphere. To inhibit the loss of arsenic from the surface during annealing the samples were capped using the face-to-face configuration with undoped GaAs.

All the Raman spectra (Sec. II B) obtained from these samples were essentially identical with those obtained from a homogeneously doped AlAs:C sample (labeled MR930), grown at the same temperature and with the same  $\text{CCl}_4$  flow rate as for the doping spikes in the superlattice sample. The doped layer was 560 nm thick and was capped with a 10 nm thick nominally undoped GaAs layer.

### B. Experimental results

Fourier transform infrared (FTIR) absorption spectra using a Bruker IFS 120 HR interferometer, operated at a resolution of  $0.5\text{ cm}^{-1}$  (sample temperature  $\sim 10\text{ K}$ ), showed a line at  $2555.7\text{ cm}^{-1}$  with a width of  $2.9\text{ cm}^{-1}$  due to the

stretch mode of H-C<sub>As</sub> pairs<sup>12</sup> in the as-grown AlAs:C  $\delta$ -doping superlattice. The measured integrated absorption (IA) coefficient of this line was used to estimate an areal concentration of  $5 \times 10^{13} \text{ cm}^{-2}$  per superlattice period, by using the calibration factor established for GaAs:H-C<sub>As</sub>.<sup>15</sup> This line was not detected in the annealed material. The LVM at  $631.3 \text{ cm}^{-1}$ , due to isolated C<sub>As</sub> acceptors, showed a Fano profile for both the as-grown and annealed samples, due to strong free carrier absorption.<sup>12</sup> FTIR measurements on the as-grown homogeneously doped sample MR930 gave a concentration of H-C<sub>As</sub> pairs of  $8.4 \times 10^{19} \text{ cm}^{-3}$ . Pieces of this material annealed for 15 min in a nitrogen atmosphere at temperatures of 500 or 600 °C had reduced values of [H-C<sub>As</sub>] of  $7.8 \times 10^{19} \text{ cm}^{-3}$  and  $1.5 \times 10^{19} \text{ cm}^{-3}$ , respectively, but after anneals at 700 and 825 °C the values of [H-C<sub>As</sub>] pairs were below the detection limit of  $1 \times 10^{18} \text{ cm}^{-3}$ . Concomitant with the initial decrease in [H-C<sub>As</sub>] on annealing there was an increase in  $p$ , measured by the van der Pauw method at room temperature, from  $5.5 \times 10^{19} \text{ cm}^{-3}$  (as-grown) to  $7.1 \times 10^{19} \text{ cm}^{-3}$  and  $1.7 \times 10^{20} \text{ cm}^{-3}$  after anneals at 500 and 600 °C, respectively. However, after the anneals at 700 and 825 °C,  $p$  decreased to  $1.4 \times 10^{20} \text{ cm}^{-3}$  and  $8.4 \times 10^{19} \text{ cm}^{-3}$ , respectively. The Hall mobility determined for the as-grown sample was  $16 \text{ cm}^2 \text{ V}^{-1} \text{ s}^{-1}$  and after annealing at 500, 600, 700, and 825 °C,  $p$  values of 15, 12, 16, and 15  $\text{cm}^2 \text{ V}^{-1} \text{ s}^{-1}$ , respectively, were obtained.

High-resolution x-ray diffraction (HRXRD) measurements carried out on the  $\delta$ -doping superlattice annealed at 600 °C showed  $\sim 9$  satellite lines on both sides of the main epilayer peak. Simulation of the diffraction profile indicated an absence of dislocations in the material and that the C concentration profiles for the  $\delta$ -doped layers were abrupt (see Ref. 16). Assuming Vegard's law to be valid and that all the carbon was present as isolated C<sub>As</sub>,<sup>17</sup> we obtained a superlattice period of 52 nm, a  $\delta$ -doped layer concentration of  $2.2 \times 10^{20} \text{ cm}^{-3}$ , and a  $\delta$ -layer width of 2.8 nm. The intensities of the satellite peaks were approximately 35% higher for the annealed material than for the as-grown sample, consistent with the higher strain associated with isolated C<sub>As</sub> acceptors compared with H-C<sub>As</sub> pairs.<sup>17</sup> However, the intensities of the satellite peaks for a piece of this wafer annealed at 850 °C were approximately 20% lower than for the as-grown sample. HRXRD measurements on the homogeneously doped sample MR930 after an anneal at 600 °C showed that the strain in the AlAs layer increased by 32% compared with the as-grown layer, due primarily to the removal of H-C<sub>As</sub> pairs. After anneals at higher temperatures this increased strain was reduced, implying loss of carbon atoms from arsenic lattice sites.

Low-temperature (77 K) Raman measurements were made in the backscattering geometry from the (100) growth surface using excitation from a Kr<sup>+</sup> ion laser ( $h\nu_L = 3.00$  or 3.05 eV) or from an Ar<sup>+</sup> laser ( $h\nu_L = 2.71$  eV). The scattered light was dispersed in a triple spectrometer and detected with a silicon charge-coupled detector (CCD) array without analyzing the polarization. The Raman spectrum of the AlAs:C  $\delta$ -doping superlattice annealed at 850 °C for 30 min is shown in Fig. 1, covering the frequency range from 1580 to 1980  $\text{cm}^{-1}$ . For comparison, a spectrum is also

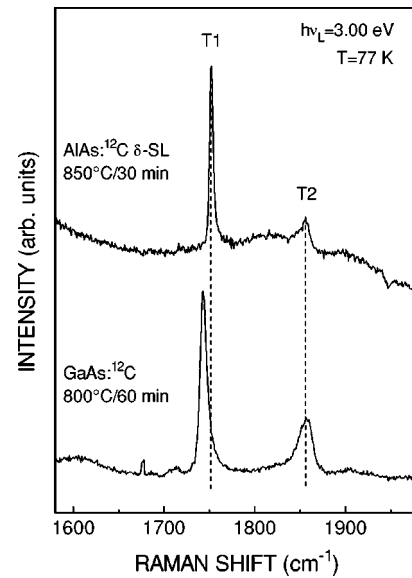


FIG. 1. Raman spectra (resolution  $2 \text{ cm}^{-1}$ ) showing a comparison of an annealed AlAs:<sup>12</sup>C  $\delta$ -doping superlattice with an annealed uniformly doped GaAs:<sup>12</sup>C sample.

shown for GaAs doped uniformly with [<sup>12</sup>C] =  $5 \times 10^{20} \text{ cm}^{-3}$  after being annealed at 800 °C for 60 min.

The two spectra were recorded using the same experimental conditions of optical excitation at 3.00 eV and spectral resolution of  $2 \text{ cm}^{-1}$ . The latter spectrum shows two lines at  $1743 \text{ cm}^{-1}$  ( $T1$ ) and  $1856 \text{ cm}^{-1}$  ( $T2$ ) previously assigned to directly bonded split-interstitial <sup>12</sup>C-<sup>12</sup>C complexes in GaAs.<sup>4</sup> The intensity of the line at  $1856 \text{ cm}^{-1}$  is weaker than that of the line at  $1743 \text{ cm}^{-1}$ , consistent with the previous results. A corresponding pair of lines at  $1752$  and  $1856 \text{ cm}^{-1}$  was detected in the annealed AlAs:C  $\delta$ -doping superlattice sample. The closeness of the frequencies and relative strengths of the two lines for the two host crystals imply that the lines detected in AlAs should also be attributed to directly bonded dicarbon complexes. The low-frequency line in AlAs ( $T1$ ) is  $\sim 9 \text{ cm}^{-1}$  higher in frequency than that in GaAs and has a full width at half maximum (FWHM) of  $5 \text{ cm}^{-1}$ , compared with  $9 \text{ cm}^{-1}$  for GaAs. The higher-frequency line ( $T2$ ) appears at essentially the same frequency for both hosts and has values of FWHM of 15 and  $19 \text{ cm}^{-1}$  for AlAs and GaAs, respectively.

To exclude the possibility that the Raman lines observed for the AlAs:C  $\delta$ -doping superlattice sample originate from the GaAs capping layer, this layer was removed from part of the sample annealed at 600 °C by selective wet chemical etching. Raman spectra then showed a fivefold increase in intensity of both the  $T1$  and  $T2$  lines. This increase is the expected value resulting from the elimination of the attenuation of the incident and scattered light on passing through the 20 nm thick GaAs capping layer.

Figure 2 shows a series of Raman spectra taken from the as-grown AlAs:C  $\delta$ -doping superlattice sample as well as from the pieces annealed at 600 °C and 850 °C, respectively. Optical excitation was again at 3.00 eV with the spectral resolution set to  $2 \text{ cm}^{-1}$ . There are increases in the scattering intensities of both the  $T1$  and  $T2$  modes upon annealing. It is clear that C-C dimers are formed during growth and their concentrations are increased during the lower-

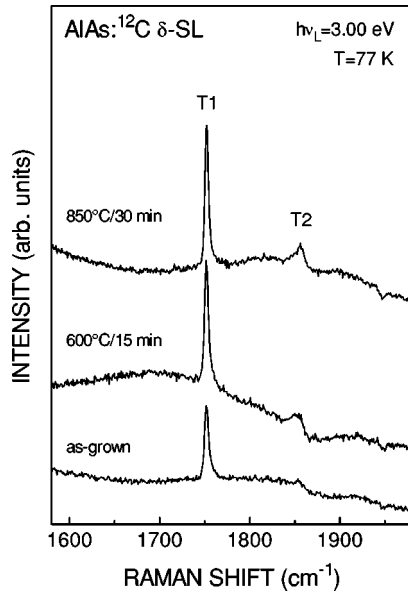


FIG. 2. Raman spectra (resolution  $2\text{ cm}^{-1}$ ) of the AlAs:C  $\delta$ -doping superlattice (see Fig. 1) in its as-grown state and following anneals at  $600^\circ\text{C}$  and  $850^\circ\text{C}$ .

temperature anneal that is used to dissociate H-C<sub>As</sub> pairs. It follows that the measured increase in the hole concentration after the  $600^\circ\text{C}$  anneal is smaller than that expected if the dissociation process were the only process that had occurred.

Raman spectra measured at excitation energies of 2.71, 3.00, or 3.05 eV (Fig. 3) show that the scattering strength of the *T2* mode, relative to that of the *T1* mode, is enhanced for excitation at 3.00 and 3.05 eV. By contrast, the *T2* line is barely detected in the Raman spectrum for optical excitation at 2.71 eV. This resonant behavior is similar to that observed for the dicarbon complex in GaAs.<sup>4</sup> It is not clear, however, whether the increase in the *T2* line intensity observed for excitation at around 3 eV is caused by a resonance with an

internal electronic transition of the dicarbon complex, or is due to the  $E_0$  band gap resonance of the AlAs, and the  $E_1$  band gap resonance of the GaAs host crystal, respectively. Both of these interband resonances occur at about 3 eV.<sup>18</sup> It is important to note that the Raman spectra are superposed on a photoluminescence (PL) background that is stronger than the *T1* Raman line by a factor of between 5 and 10. Thus the *apparent* shape of the weaker *T2* line (see Fig. 3) depends on the smoothness of this PL background. The spectral shape of this background can be distorted by small (maximum of 5% to 10%) variations in the sensitivity of the elements of the CCD detector array.

Further Raman measurements on the carbon  $\delta$ -doping superlattice AlAs sample annealed at  $850^\circ\text{C}$  were carried out as a function of excitation power density over the range  $1 \times 10^3$  to  $1 \times 10^4\text{ W cm}^{-2}$  at an incident photon energy of 3.00 eV. The intensities of the *T1* and *T2* modes both showed linear increases with increasing excitation power, to within the noise limits of the measurement. The same dependence was found for an annealed homogeneously doped AlAs epilayer. As the ratio of the intensities of the *T1* and *T2* modes is essentially constant, within the measurement errors, and is independent of the carrier concentration for the samples examined, there is the possibility that both modes originate from the same defect. It is established that *T1* and *T2* are due to directly bonded dicarbon complexes and, if they are due to compensating centers, they would be present in the positive charge state in the present *p*-type samples. The concentration of photogenerated electron-hole pairs is not expected to raise the position of the Fermi level when the samples are illuminated by the laser radiation because of the high background hole concentrations; thus no changes are to be expected in the charge states of the dimers. In the following section we therefore investigate the charge state and vibrational frequencies of dimer defects located in various sites, paying particular attention to centers that act as donors or deep hole traps.

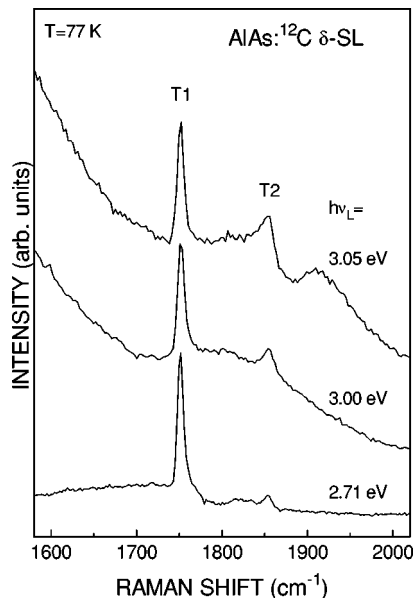


FIG. 3. Raman spectra (resolution  $6\text{ cm}^{-1}$ ) of the annealed ( $850^\circ\text{C}$ ) AlAs:C  $\delta$ -doping superlattice excited at various photon energies as given in the figure.

### III. THEORETICAL MODELING

#### A. Method

*Ab initio* calculations were carried out using a density functional cluster method (*Aimpro*) which gives the total energy of H-terminated atomic clusters. Norm-conserving pseudopotentials<sup>19</sup> are used to eliminate the core electrons on C, Ga, Al, and As nuclei. The Kohn-Sham wave functions are expanded in a basis set of *s* and *p* Gaussian orbitals. The basis set consisted of four Gaussian-type orbitals in *s*, *p<sub>x</sub>*, *p<sub>y</sub>*, *p<sub>z</sub>* variants, with different widths, centered on each aluminum, arsenic, and carbon atom, with two Gaussian orbitals per hydrogen atom. The required orbital symmetries of the basis functions are provided by suitable multiplicative factors. The charge density was fitted to five *s*-type Gaussian functions for each aluminum and arsenic atom, four for each carbon, and three for each hydrogen. Additional Gaussian-type basis functions were placed at the center of every bond, except to the terminating hydrogen atoms. The H atoms were also described with a fixed linear combination of Gaussian orbitals. All calculations used a spin-averaged exchange-correlation energy functional, with a modified interpolation scheme for the Ceperley-Alder expression, which does not

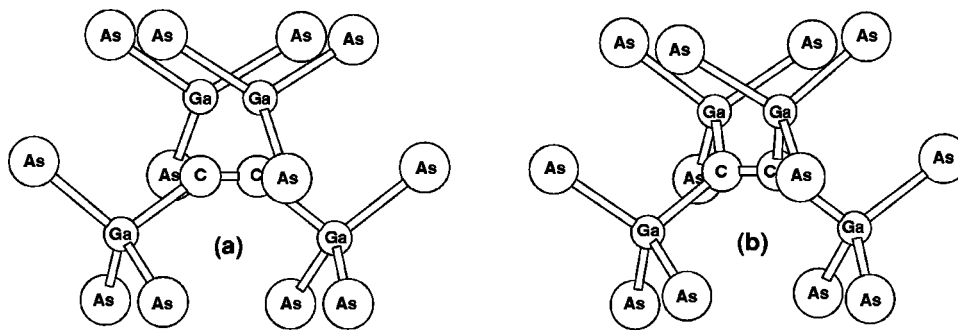


FIG. 4. (a) The [110]-aligned  $(C-C)_{As}^+$  complex, (b) the [100]-aligned  $(C-C)_{As}^0$  complex. The group III atoms are shown as Ga; they are interchangeable with Al.

appear to suffer from the overbinding usually seen in the local density approximation (LDA) method.<sup>20</sup> The forces acting on each atom are given by an analytical formula derived from the total energy expression. Structural optimization to minimize the total energy is performed by a conjugate-gradient algorithm, either with or without imposing a selected symmetry. Further details are given in a recent review.<sup>21</sup> The method has previously been used to explore C and C-H defects in GaAs and AlAs and their alloys<sup>5,22–25</sup> as well as carbon dimers in GaAs.<sup>4</sup>

The carbon dimer in AlAs was inserted into a 71-atom tetrahedral cluster replacing the central As atom to give a resulting composition  $C_2Al_{16}As_{18}H_{36}$ . This cluster was relaxed until the residual forces were negligible for both the neutral and singly ionized charge states of the C-C pair that was initially oriented along the [100] direction with  $D_{2d}$  symmetry. The LVMs associated with displacements of the six central atoms of the defect complex were then calculated.<sup>4</sup> Similar investigations were made for dicarbon pairs occupying a group III lattice site with a similar sized cluster but with the condition that the dimer occupied the central site. Calculations were also carried out for interstitial dimers with various configurations. Finally, additional calculations were made with a larger cluster of 132 atoms, allowing full variational freedom over all atoms except hydrogen, for selected defects, leading to essentially similar results.

The calculated values for the vibrational frequencies presented here have two main sources of error. First, they are very sensitive to the equilibrium bond length. A 3% increase lowers the mode frequency by 10%,<sup>26</sup> so that an error of less than 0.04 Å in the length of the C-C bond changes the frequency of its stretch mode by more than 150  $cm^{-1}$ . The second, smaller, source of error arises since restoring force constants are found by determining the change in energy for an atom displaced from its equilibrium position by  $\sim 0.1$  Å. These force constants do not take account of all anharmonic effects. Nevertheless, previous experience indicates that discrepancies between calculated and measured frequencies are usually no greater than about 10%.

Finally, the calculated frequencies for the dimer in AlAs or GaAs are expected to be broadly comparable with the measured frequencies for the molecule in the gas phase providing there is a similar charge density in the C-C bond. Comparisons can be made with the frequencies of 1351, 1855, and 1781  $cm^{-1}$  for the positive, neutral, and negative charge states of the  $^{12}C_2$  molecule.<sup>27,28</sup> Further comments are made in Sec. IV.

### B. Results for $(C-C)_{As}$

Our earlier theoretical work on GaAs used an equivalent basis to that defined above but with gallium replacing alumi-

num. To facilitate comparison with the current work, we first repeated the GaAs calculations, paying particular attention to minimize residual atomic forces by increasing the number of iterations. Initially, the relaxation was carried out by imposing  $D_{2d}$  symmetry, as in the earlier analysis.<sup>4</sup> The present calculation led to a slightly lower frequency of 1764  $cm^{-1}$ , compared with 1798  $cm^{-1}$  obtained previously for the LVM of the  $^{12}C$ - $^{12}C$  positively charged [100]-oriented dimer. However, further investigation, without the imposition of any symmetry constraint, showed that the [100]- $(C-C)_{As}^+$  defect in either AlAs or GaAs was unstable following a small “random” displacement of the initial atomic coordinates sufficient to break the  $D_{2d}$  symmetry. Relaxation led to C-C pairs aligned approximately parallel to a [110] direction and displaced slightly in the [001] direction away from the center of the As vacancy [down in Fig. 4(a)]. These configurations had energy minima lower by 0.54 eV for AlAs and 0.45 eV for GaAs, compared with the [100]- $(C-C)_{As}^+$  orientation. The resulting symmetry is very close to, but not exactly  $C_{2v}$ , and there are two deep empty levels that are close together and slightly above midgap.

This changed orientation leads to a slight shortening of the C-C bond and, as a consequence, the stretch modes of the  $^{12}C$ - $^{12}C$  defects have higher calculated frequencies of 1955  $cm^{-1}$  in AlAs and 1950  $cm^{-1}$  in GaAs (Table I). The induced dipole moment of the  $^{12}C$ - $^{12}C$  stretch mode for each host was determined by finding the change in the cluster dipole moment when the atoms were displaced according to the appropriate normal coordinate. Since large displacements occur only for the carbon atoms, these moments are almost zero and the modes are not expected to be infrared active. Other vibrational modes of the cluster occur at frequencies below 500  $cm^{-1}$ . These modes were not detected by infrared absorption because of strong free carrier absorption and neither were they detected by Raman scattering.

Further simulations made using other choices for the initial atomic coordinates produced a stable  $(C-C)_{As}^+$  complex with the C-C bond aligned a few degrees off the  $\langle 111 \rangle$  direction. This complex has essentially the same energy and frequency as the  $\langle 110 \rangle$ -oriented dimer. The final alignment varied slightly depending on the initial choice of coordinates before relaxation, as did the frequency of the fundamental C-C stretch mode, since the energy surface is rather flat around this orientation. For this defect the two C atoms are inequivalent, leading to a splitting of the mixed isotope  $^{12/13}C$  modes in AlAs of  $\sim 4$   $cm^{-1}$ ; in GaAs the splitting is about half this value. Such a splitting for GaAs would not have been detected (see Sec. I) and measurements were not made on AlAs containing the mixed isotopes.

TABLE I. Calculated and measured LVM frequencies ( $\text{cm}^{-1}$ ) and bond lengths ( $\text{\AA}$ ) for dicarbon defects in AlAs and GaAs.

			$^{12}\text{C}-^{12}\text{C}$	$^{12}\text{C}-^{13}\text{C}$	$^{13}\text{C}-^{13}\text{C}$	C-C
[110]-AlAs:(C-C) $_{\text{As}}^+$			1955	1917	1878	1.23
[110]-GaAs:(C-C) $_{\text{As}}^+$			1950	1912	1873	1.22
[111]-AlAs:(C-C) $_{\text{As}}^+$			1948	1912, 1908	1871	1.23
[111]-GaAs:(C-C) $_{\text{As}}^+$			1943	1908, 1903	1867	1.23
[100]-AlAs:(C-C) $_{\text{As}}^0$			1599	1568	1536	1.29
[100]-GaAs:(C-C) $_{\text{As}}^0$			1590	1559	1527	1.28
[100]-AlAs:(C-C) $_{\text{As}}^+$	(constrained $D_{2d}$ )		1806	1771	1735	1.25
[100]-GaAs:(C-C) $_{\text{As}}^+$	(constrained $D_{2d}$ )		1764	1729	1694	1.25
[110]-AlAs:(As-C-C-As) $_i^{2+}$			1930	1893	1855	1.24
[110]-GaAs:(As-C-C-As) $_i^{2+}$			1975	1936	1897	1.23
[110]-AlAs:(Al-C-C-Al) $_i^{2+}$			1804	1769	1733	1.26
[110]-GaAs:(Ga-C-C-Ga) $_i^{2+}$			1870	1834	1797	1.25
[110]-AlAs:(Al-C-C-Al) $_i^0$			1769	1736	1700	1.29
[110]-GaAs:(Ga-C-C-Ga) $_i^0$			1746	1712	1678	1.29
Observed	AlAs:	$T_1$	1752			
Observed	GaAs:	$T_1$	1743 <sup>a</sup>	1708 <sup>b</sup>	1674 <sup>b</sup>	
Observed	AlAs:	$T_2$	1856			
Observed	GaAs:	$T_2$	1856 <sup>a</sup>	1824 <sup>b</sup>	1788 <sup>b</sup>	

<sup>a</sup>Previous values were  $1749 \text{ cm}^{-1}$  and  $1859 \text{ cm}^{-1}$ .

<sup>b</sup>From previous work. See Ref. 4.

We also considered a  $(\text{C-C})_{\text{As}}^+$  dimer with a  $\langle 110 \rangle$  orientation perturbed by a vacancy,  $V_{\text{As}}^{2+}$  at the next nearest neighbor As site, as a vacancy could have been generated as a result of a  $\text{C}_{\text{As}}$  atom migrating from its As site during annealing (as stated in Sec. I). The calculated length of  $1.226 \text{ \AA}$  of the C-C bond (using a 131-atom cluster) was essentially unchanged as a result of the perturbation, implying that the associated vibrational frequency would be unchanged (Table I).

For completeness, we also examined the neutral  $(\text{C-C})_{\text{As}}$  defect when the doubly degenerate deep level in the gap is singly occupied. The  $\langle 110 \rangle$ -oriented state was unstable, and spontaneously relaxed to a configuration close to the  $\langle 100 \rangle$ -aligned structure in both AlAs and GaAs [Fig. 4(b)] (Table I). If the defect had  $D_{2d}$  symmetry in this charge state, the two associated gap levels would be degenerate. However, a Jahn-Teller distortion lowers the symmetry, thereby splitting the levels and lowering the total energy by about  $0.4 \text{ eV}$ .

### C. Results for $(\text{C-C})_{\text{III}}$

Although it is unlikely that  $(\text{C-C})_{\text{III}}$  defects will be present, since  $\text{C}_{\text{Ga}}$  or  $\text{C}_{\text{Al}}$  donors have not been detected, calculations have been made for carbon dimers occupying group III lattice sites as these defects are triple donors. The uppermost level is well above midgap and would be empty in heavily doped  $p$ -type material. The next lower level, that has a deep state in the bottom half of the gap, may be either unoccupied or only singly occupied. The singly ionized state (+1) state may lead to dimer alignments parallel to either  $\langle 100 \rangle$  or  $\langle 110 \rangle$  directions, since the energies of the two configurations are nearly degenerate. Nevertheless, they have

very different frequencies of  $1519 \text{ cm}^{-1}$  and  $2044 \text{ cm}^{-1}$ , respectively. In the +2 and +3 ionized states the C-C frequencies are slightly greater than  $2000 \text{ cm}^{-1}$  and the alignments are nearly parallel to  $[110]$ .

### D. Results for $(\text{C-C})_i$

The dimer placed at a  $T_d$  interstitial site in a  $\text{C}_2\text{M}_{16}\text{As}_{19}\text{H}_{36}$  ( $M = \text{Al}$  or  $\text{Ga}$ ) cluster surrounded by a cage of four As atoms was also investigated. This structure would be expected to possess almost identical C-C stretch modes in GaAs and AlAs as found experimentally. The neutral dimer was initially assumed to have  $D_{2d}$  symmetry, but a lower-energy site was found by displacing the dimer away from the  $T_d$  site. For arbitrary displacements, both neutral and ionized C-C pairs moved spontaneously towards the midpoint of a nearby lattice bond. The relaxed complex has an occupied level which appears in the lower half of the gap and therefore would be doubly ionized in  $p$ -type crystals. One of the C atoms adopted a nearly bond-centered configuration, while the other was located in the general direction of one of the surrounding host atoms. The resulting structure has inequivalent carbon atoms but is not in conflict with the observation of a ‘‘single’’ mode from the  $^{12}\text{C}-^{13}\text{C}$  pairs.<sup>4</sup> This is because the calculated splitting of the frequencies of the  $^{12}\text{C}-^{13}\text{C}$  modes was only  $\sim 2 \text{ cm}^{-1}$  that would not have been resolved experimentally. Specifically, calculations for GaAs yielded a  $^{12}\text{C}-^{12}\text{C}$  mode at  $1983 \text{ cm}^{-1}$ ,  $^{12}\text{C}-^{13}\text{C}$  modes at  $1945.7 \text{ cm}^{-1}$  and  $1943.9 \text{ cm}^{-1}$ , and a  $^{13}\text{C}-^{13}\text{C}$  mode at  $1905 \text{ cm}^{-1}$ .

We then investigated the  $[110]$ - $(\text{C-C})_{\text{As}}$  complex [Fig. 4(a)], with an additional As atom lying in the same plane as the carbon pair and its two Al or Ga neighbors, and along the

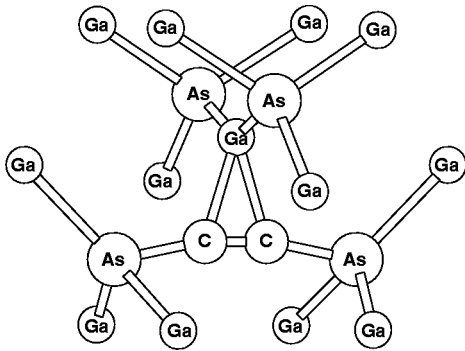


FIG. 5. The [110]-aligned,  $C_{2v}$   $(C-C)_i^{2+}$  complex. The group III atoms are shown as Ga; they are interchangeable with Al. This structure is  $\approx 0.6$  eV lower in energy than when the group III and As atoms are transposed.

[001] direction perpendicular from the midpoint of the C-C bond, with  $C_{2v}$  symmetry. For the neutral state the highest occupied level lies slightly above the valence band edge, so that the defect could be ionized. In GaAs, the neutral and doubly ionized states have  $^{12}\text{C}-^{12}\text{C}$  modes at  $1870\text{ cm}^{-1}$  and  $1746\text{ cm}^{-1}$ , respectively. However, the corresponding modes in AIAs have frequencies higher by  $\sim 100\text{ cm}^{-1}$  than in GaAs due to the lighter mass of Al atoms than Ga atoms, contrary to the experimental observations. Furthermore, the interstitial dicarbon complex with inequivalent C atoms to be described below is at least 0.6 eV lower in energy. These dicarbon-arsenic interstitial complexes can therefore be excluded.

Closer examination of the complex with inequivalent carbon atoms revealed that it is a distorted form of the complementarity structure to the  $C_{2v}$  symmetry interstitial pair, i.e., with the identities of the group III and the As atoms transposed (see Fig. 5). The distortion was simply the result of an accidental local minimum in the energy. In a  $\text{C}_2\text{Al}_{19}\text{As}_{16}\text{H}_{36}$  cluster with  $C_{2v}$  symmetry the  $^{12}\text{C}-^{12}\text{C}$  mode of the doubly ionized center was found to be  $1930\text{ cm}^{-1}$ . The frequency in the corresponding GaAs case is slightly higher at  $1975\text{ cm}^{-1}$ . This difference was smaller ( $18\text{ cm}^{-1}$ ) in the previous calculation where the structure was distorted, thus illustrating the sort of variation which is usually found. As the carbon atoms are now equivalent in the cluster with  $C_{2v}$  symmetry, there is no splitting of the mixed isotope lines.

#### IV. ASSIGNMENTS OF RAMAN LINES

Raman scattering measurements on as-grown and annealed samples of AIAs:C show LVMS with frequencies close to those detected previously in annealed GaAs:C and assigned to dicarbon complexes: it should be noted that these frequencies are close to those found for gaseous dicarbon molecules (see Sec. I). The frequency differences between the modes  $T1$  and  $T2$  are  $113\text{ cm}^{-1}$  and  $104\text{ cm}^{-1}$  for GaAs and AIAs, respectively. Previously, it was suggested that the higher-frequency line ( $T2$ ) of GaAs might be a combination of a stretch mode and a low-frequency defect mode lying in the spectral region of the acoustic lattice modes.<sup>4</sup> We now reject this interpretation since a larger frequency difference would be expected for AIAs than for GaAs due to the lighter group III mass, whereas the separation is actually smaller.

We now discuss the sites and orientations of dicarbon complexes that would give two modes that have similar frequencies according to the *ab initio* calculations, to within an uncertainty of about 10% (see Table I).

It is most likely that carbon dimers are present as  $(C-C)_{\text{As}}$  since the first carbon atom will already be present on an arsenic lattice site and the pair defect will be formed by the capture of a migrating interstitial carbon atom (initially first order kinetics). On the other hand, the formation of interstitial dicarbon centers would require two interstitial carbon atoms to combine as a result of their diffusion (second order kinetics). The assignment of  $T1$  and  $T2$  to the substitutional and interstitial centers would lead to a perceived difficulty: since two different diffusion processes would have to be invoked, it would be difficult to explain the essentially constant ratio of the strengths of the  $T1$  and  $T2$  centers (for both GaAs and AIAs) throughout the whole annealing process. Although the calculated frequencies could offer an explanation of the observations, we nevertheless reject this interpretation. The essentially constant ratio of the strengths of the  $T1$  and  $T2$  centers also argues against the assignment of the two triplets to a substitutional dicarbon complex that is either isolated or perturbed by another defect, such as an adjacent arsenic vacancy. Consequently, we do not consider the latter defects further.

*Ab initio* calculations have been carried out for both positively charged and neutral  $(C-C)_{\text{As}}$  centers but in heavily *p*-doped material the defects will be in the positive charge state and the laser irradiation is not expected to induce a change to the neutral state. The dependence of the strengths of the two modes on laser power was found to be linear in AIAs over an order of magnitude change in the excitation power density at 3.00 eV, although the corresponding modes in GaAs showed increases of only a factor of about 2 for an increase in power of a factor of 3.<sup>4</sup> This small difference for the two host crystals may occur because AIAs and GaAs have indirect and direct band gaps, respectively. Thus, the penetration depth of the incident light is much greater in AIAs than in GaAs, so that the density of photogenerated carriers is at least an order of magnitude greater in GaAs than in AIAs. It should be noted, however, that for GaAs there is some evidence for band bending due to the presence of surface states just above the top of the valence band<sup>29</sup> that might reduce the density of holes in this region. Finally, the high absorption coefficient for GaAs may lead to a higher local temperature compared with AIAs and this may reduce the strength of the Raman signal: these lines are not observed for measurements made on samples held at room temperature. Laser powers smaller than those quoted in Sec. II B could not be used since the signal to noise ratio was unacceptably small. In summary, no evidence was found for changes in the charge states of the complexes under investigation resulting from optical excitation in either AIAs or GaAs.

It follows that the comparison should be made between the observations and theoretical predictions relating to various orientations of the positively charged dicarbon located on an arsenic lattice site. Calculated energies for [110]- $(C-C)_{\text{As}}^+$  and [111]- $(C-C)_{\text{As}}^+$  are essentially indistinguishable, whereas the energy for [100]- $(C-C)_{\text{As}}^+$  ( $D_{2d}$  symmetry imposed) is higher by about 0.5 eV. Since  $T1$  and

$T2$  are observed simultaneously, it is inferred that the difference of their configurational energies cannot be significantly greater than the value of  $kT$  at room temperature (approximately 0.025 eV). Consequently, the  $[100]$ -(C-C) $_{As}^+$  orientation is not considered further. To achieve equilibrium, the magnitude of the barrier between any two configurations must be small. Calculations indicate that there is a flat potential surface around both the  $[110]$ -(C-C) $_{As}^+$  and  $[111]$ -(C-C) $_{As}^+$  orientations, consistent with this requirement. The two calculated frequencies are 1950 and 1943  $\text{cm}^{-1}$ , respectively, for GaAs and 1955 and 1948  $\text{cm}^{-1}$  for AlAs. The uncertainties in the calculations are too large ( $\sim 200 \text{ cm}^{-1}$  or 10%) to permit unambiguous assignments to  $T1$  and  $T2$  in either host crystal.

The predictions of our *ab initio* cluster calculations show important differences with the theoretical work of Cheong and Chang.<sup>6</sup> They found, using a plane-wave soft-pseudopotential method, that the  $[100]$  orientation, attributed to a double bonded (C-C) $_{As}$  pair, was the lowest energy for both the positive and neutral charge states. They also found that the C-C bond length was significantly longer at 1.33 Å. Such a long bond length is incompatible with the high vibrational frequencies which are observed. In addition, there cannot be a double bond between the C atoms as the pair of back bonds on one C atom lies in an orthogonal plane to the second C atom. Furthermore, the additional electron in the neutral defect occupies an  $e$  orbital which must impose a small Jahn-Teller distortion on the  $D_{2d}$  symmetry of the  $[100]$  oriented dimer. No distortion was reported.

## V. CONCLUSIONS

The Hall and HRXRD results demonstrate that annealing heavily carbon-doped AlAs at temperatures above 600 °C causes a reduction in the free carrier concentration and strain. This is not related to the presence of H-C $_{As}$  pairs but is due to reductions in the concentrations of isolated C $_{As}$  acceptors because of supersaturation that leads to the formation of carbon complexes. Raman scattering measurements made on as-grown and annealed heavy carbon-doped AlAs have revealed two modes ( $T1$  at 1752  $\text{cm}^{-1}$  and  $T2$  at 1856  $\text{cm}^{-1}$ )

that are directly comparable with lines assigned to vibrational modes of directly bonded dicarbon defects at As sites in GaAs. One of these modes ( $T2$ ) shows resonant behavior relative to the other mode with excitation at an energy of 3 eV, similar to that found in GaAs.

Theoretical investigations have located an interstitial site for the dicarbon defect that acts as a deep double donor for which the predicted splitting between the modes for mixed isotope defects is negligible. Assignment of either  $T1$  or  $T2$  to this defect is excluded since the concentration of these defects is expected to depend on the details and annealing history of samples, contrary to the experimental observations. The possibility that the  $T1$  and  $T2$  modes should be assigned to one of the positively charged substitutional centers and the neutral substitutional dimer, aligned along a  $[100]$  direction, is also rejected, as the concentration of photogenerated electron-hole pairs is not expected to raise the position of the Fermi level because of the high background hole concentrations and no evidence was found for changes in the charge state of the centers resulting from increasing the laser power. However, the *ab initio* calculations have shown that the positively charged dicarbon complex, located on a substitutional arsenic lattice site, has two orientations with similar energies and vibrational frequencies. The carbon atoms are equivalent ( $\langle 110 \rangle$  axis), or closely equivalent ( $\langle 111 \rangle$  axis) and both centers are deep donors. The possibility that the defect can be present in these two orientations offers an explanation for the observation of the two dicarbon Raman modes. Nevertheless, the uncertainties in the calculated frequencies precludes assignments of  $T1$  or  $T2$  being made to a particular orientation.

## ACKNOWLEDGMENTS

The Engineering and Physical Sciences Research Council (EPSRC), UK, is thanked for its financial support at Exeter University (Contract No. GR/L34457), Imperial College (Contract No. GR/K96977), and Sheffield University (Contract No. GR/K96977). J. W. thanks G. Weimann for continuing support.

\*Electronic address: b.davidson@ic.ac.uk

<sup>1</sup>C. R. Abernathy, in *State-of-the-art Program on Compound Semiconductors, XXIV*, edited by F. Ren, S. J. Pearton, S. N. G. Chu, R. J. Shul, W. Pletschen, and T. Kamijo (The Electrochemical Society, Pennington, NJ, 1996), Vol. 96-2, pp. 1–18, and references therein.

<sup>2</sup>H. Fushimi and K. Wada, *J. Appl. Phys.* **82**, 1208 (1997).

<sup>3</sup>S. P. Westwater and T. J. Bullough, *J. Cryst. Growth* **170**, 752 (1997).

<sup>4</sup>J. Wagner, R. C. Newman, B. R. Davidson, S. P. Westwater, T. J. Bullough, T. B. Joyce, C. D. Latham, R. Jones, and S. Öberg, *Phys. Rev. Lett.* **78**, 74 (1997).

<sup>5</sup>R. Jones and S. Öberg, *Mater. Sci. Forum* **143-147**, 253 (1994).

<sup>6</sup>Byoung-Ho Cheong and K. J. Chang, *Phys. Rev. B* **49**, 17436 (1994).

<sup>7</sup>M. Sugimoto, I. Ogura, H. Saito, A. Yasuda, H. Kosaka, T. Numai, and K. Kasahara, *J. Cryst. Growth* **127**, 1 (1993).

<sup>8</sup>K. Watanabe and H. Yamazaki, *J. Appl. Phys.* **72**, 4975 (1992).

<sup>9</sup>K. Watanabe and H. Yamazaki, *J. Appl. Phys.* **74**, 5587 (1993).

<sup>10</sup>C. R. Abernathy, J. D. Mackenzie, W. S. Hobson, and P. W. Wisk, *Appl. Phys. Lett.* **65**, 2205 (1994).

<sup>11</sup>J. D. Mackenzie, C. R. Abernathy, S. J. Pearton, and S. N. G. Chu, *Appl. Phys. Lett.* **66**, 1397 (1995).

<sup>12</sup>B. R. Davidson, R. C. Newman, R. E. Pritchard, D. A. Robbie, M. J. L. Sangster, J. Wagner, A. Fischer, and K. Ploog, *Mater. Sci. Forum* **143-147**, 247 (1994).

<sup>13</sup>R. J. Malik, J. Nagle, M. Micovic, R. W. Ryan, T. Harris, M. Geva, L. C. Hopkins, J. Vandenberg, R. Hull, R. E. Kopf, Y. Anand, and W. Braddock, *J. Cryst. Growth* **127**, 686 (1993).

<sup>14</sup>A. Mazuelas, R. Hey, B. Jenichen, and H. T. Grahn, *Appl. Phys. Lett.* **70**, 2088 (1997).

<sup>15</sup>B. R. Davidson, R. C. Newman, T. B. Joyce, and T. J. Bullough, *Semicond. Sci. Technol.* **11**, 455 (1996).

<sup>16</sup>B. R. Davidson, L. Hart, R. C. Newman, T. B. Joyce, T. J. Bullough, and C. C. Button, *J. Mater. Sci.: Mater. Electron.* **7**, 355 (1996).



- <sup>17</sup>L. Hart, B. R. Davidson, J. M. Fernández, R. C. Newman, and C. C. Button, *Mater. Sci. Forum* **196-201**, 409 (1995).
- <sup>18</sup>W. Richter, in *Solid State Physics*, edited by G. Höhler and E. A. Niekiesch (Springer, Berlin, 1976), p. 121.
- <sup>19</sup>G. B. Bachelet, D. R. Hamann, and M. Schlüter, *Phys. Rev. B* **26**, 4199 (1982).
- <sup>20</sup>M. I. Heggie, C. D. Latham, S. C. P. Maynard, and R. Jones, *Chem. Phys. Lett.* **249**, 485 (1995).
- <sup>21</sup>R. Jones and P. R. Briddon, in *Identification of Defects in Semiconductors*, edited by M. Stavola, *Semiconductors and Semimetals Vol. 51A* (Academic Press, Boston, 1998), Chap. 6, p. 287.
- <sup>22</sup>R. Jones and S. Öberg, *Phys. Rev. B* **44**, 3673 (1991).
- <sup>23</sup>R. Jones and S. Öberg, *Phys. Rev. B* **49**, 5306 (1994).
- <sup>24</sup>R. E. Pritchard, B. R. Davidson, R. C. Newman, T. J. Bullough, T. B. Joyce, R. Jones, and S. Öberg, *Semicond. Sci. Technol.* **9**, 140 (1994).
- <sup>25</sup>S. J. Breuer, R. Jones, P. R. Briddon, and S. Öberg, *Phys. Rev. B* **53**, 16289 (1996).
- <sup>26</sup>J. P. Goss, R. Jones, S. Öberg, and P. R. Briddon, *Phys. Rev. B* **55**, R15576 (1997).
- <sup>27</sup>K. P. Huber and G. Herzberg, *Molecular Spectra and Molecular Structure*, edited by G. Herzberg (Van Nostrand Reinhold, New York, 1979), p. 114.
- <sup>28</sup>W. Weltner and R. J. van Zee, *Chem. Rev.* **89**, 1713 (1989).
- <sup>29</sup>M. D. Pashley, K. W. Haberern, R. M. Feenstra, and P. D. Kirchner, *Phys. Rev. B* **48**, 4612 (1993).